Original Article

Indian Journal of Forensic Medicine and Pathology
Volume 13 Number 3, July - September 2020
DOI: http://dx.doi.org/10.21088/ijfmp.0974.3383.13320.1

Ultrastructure of Cerebral Cortex Investigation during Early Postmortem Changes in a Rat Model

Ahmed Medhat Hegazy[1], Soad M Nasr[2], Sekena H Abdel Aziem[3]

How to cite this article:
Ahmed Medhat Hegazy, Soad M Nasr, Sekena H Abdel-Aziem. Ultrastructure of Cerebral Cortex Investigation during Early Postmortem Changes in a Rat Model. Indian J Forensic Med Pathol. 2020;13(3):365–375.

Abstract

Estimation of the postmortem interval (PMI) is a very essential task for forensic experts, especially in criminal cases. The PMI is the time passed since the death of an individual and refers to the stages of autolysis. The current study was designed to estimate PMI by determination of the oxidative markers, RNA integrity, GAPDH mRNA level in the brain of adult male albino rats and the autolytic ultrastructure changes of the cerebrum at time of death (0 hour), and then on 1st, 2nd, 4th, and 6th hours postmortem (hpm). Thirty-five male albino Wistar rats were included in the present study (Seven rats for each time). The results revealed a significant time-dependent malondialdehyde elevation with a decrease the antioxidant CAT, SOD, and GSH started from the 1st till the 6th hpm. On the other hand, the brain tissue GAPDH-mRNA gene expression level showed a significant decrease at the 1st and the 6th hpm. The ultrastructure changes showed significant autolytic changes in the nerve cell, the nerve axon, and the blood vessels starting from the 1st till the 6th hpm. In conclusion, oxidative markers and ultrastructure examination of the brain tissue especially cerebrum could be helpful for determination the early postmortem interval time.

Keywords: Postmortem; Oxidant/Antioxidant status; Molecular; Ultrastructure; Brain.

Introduction

The postmortem interval (PMI) is a significant focal point of examination in forensic medicine.[1] There are some factors that affect the postmortem process and make the determination of PMI difficult such as age, sex, physical, and physiological state of the deceased. In addition, there are external factors including environmental temperature and humidity as well as animal and insect activity.[2]

Different techniques have been proposed to estimate the time since death by chemical techniques, prompting the appearance of a scope called "Thanatochemistry" where all chemical changes can be evaluated after death.[3]

Decomposition starts ~4 min after death by autolysis. The cells will be gradually destroyed. As a result, liberation and damage in cellular components and metabolites occur.[4] There is a continuous release of free radicals in living tissue, which are scavenged by antioxidant systems. Post-mortem, oxidant/antioxidant balance cannot be controlled by the body, prompting biochemical aggravations.[5]

Molecular alterations in protein, DNA and RNA degradation are disentangled to give a more exact assurance of PMI.[6] The RNA is believed to be more

Authors Affiliation: [1]Lecturer, Department of Forensic Medicine and Toxicology, Faculty of Veterinary Medicine, Aswan University, P.O. Box 81528 Aswan, [2]Department of Parasitology and Animal Diseases, Veterinary Research Division, National Research Centre, [3]Department of Cell Biology, Genetic Engineering and Biotechnology Research Division, National Research Centre, 33 Bohouth Street, Post Box 12622, Dokki, Giza, Egypt.

Corresponding Author: Ahmed Medhat Hegazy, [1]Lecturer, Department of Forensic Medicine and Toxicology, Faculty of Veterinary Medicine, Aswan University, P.O. Box 81528 Aswan, Egypt.

E-mail: ahmed_medhat012@yahoo.com

susceptible to disintegration than protein and DNA. If RNA disintegration after death, tissues could be determined quantitatively. This could help in the exact determination of the PMI.[7]

So that, the goal of this research was to study the early biochemical, molecular and ultrastructure postmortem changes in the rat's brain at 0-hour, the 1st, 2nd, 4th, and the 6th-hour postmortem (hpm). The oxidant/antioxidant markers, RNA integrity, and changes in the cell organelles using an electron microscope were also investigated.

Material and Methods

Animals

Male albino Wistar rats (5 weeks old, 120–140 g weight), were obtained from the Animal House, National Cancer Institute, Egypt. Prior to the experiment, the animals were kept in cages and given a standard diet and water ad libitum. All rats were exposed to a normal light/dark cycle and room temperature (23±2 ^{o}C).

Experimental design

A total of 35 male Wistar rats were arbitrarily dispensed into five groups (7 rats each): the control group (G1) that was sacrificed and the brain tissue was taken immediately after death (0- hour). The G2, G3, G4, and G5 were sacrificed and the brain tissue was taken at the 1st, 2nd, 4th, and 6th hpm, respectively. Brain specimens were collected from all rats at the particular time of the experiment (at room temperature 25^{o}C) for estimation of the oxidant/antioxidant markers, gene expression and the changes in the cell organelles using the electron microscope.

Determination of oxidant/antioxidant markers in brain homogenates

Preparation of brain homogenate and Assay techniques

Brain tissue homogenates were prepared according to the method of Hegazy et. al.[8] Determination of the activities of catalase (CAT),[9] superoxide dismutase (SOD),[10] and the levels of reduced glutathione (GSH),[11] lipid peroxidation by-products (as malondialdehyde; MDA)[12] and the total protein content[13] were performed in the brain homogenates.

All the oxidant/antioxidant markers were measured using a spectrophotometer (Model, JASCO 7800, UV/VIS, Japan).

Determination of RNA integrity in brain tissue

RNA Extraction and cDNA Synthesis

The brain specimenswere taken at 0, 1, 2, 4 and 6 hpm then stored at -80°C. Frozen brain samples were crushed and homogenized in 1 ml Trizol solvent (Invitrogen, USA) and the total RNA was extracted according to the manufacturer's commands. The yield and quality of RNA was analyzed using NanoDrop™ 1000 spectrophotometer (Thermo Fisher Scientific, USA). The RNA integrity and degree of deterioration are assessed by agarose gel electrophoresis. The RNA (2 µg) was treated with an RNase-free DNase kit (Promega) to remove any genomic DNA contamination and cDNA turned into synthesized using PreMix cDNA Kit supplied from iNtRON Biotechnology, Korea in keeping with the producer's instructions.

Real-Time PCR Analysis

Three genes Glyceraldehyde-3-phosphate dehydrogenase (GAPDH), endogenous control, were used in the present study. The primer sequences of GAPDH (target gene) with accession number NM_001289726.1 and β-actin (reference gene) with accession number J00691 as follows:

GAPDH	F:5'- AACTTTGGCATTGTGGAAGG -3',
	R: 5'- ACACATTGGGGGTAGGAACA -3'
β-actin	F: 5′-TGTTGTCCCTGTATGCCTCT-3′
	R: 5′-TAATGTCACGCACGATTTCC-3

A negative control sample was included. The thermal Real-time polymerase chain reaction (PCR) was performed in Strata gene Mx3005P Real-Time PCR System (Agilent Technologies) in a 20 µl reaction. Each 20 µL PCR cocktail contained one µl cDNA, 10 µl TOP real TMqPCR 2X Pre MIX (SYBR Green with low ROX) (Enzynomics), 0.75 µl of forward primer (10 pmol), 0.75 µl of reverse primer (10 pmol) and 7.5 µl ddH2O. Amplification conditions included 15 min at 95°C, followed by 40 cycles at 95°C for 15 sec, at 60–63°C for 15 sec and 72°C for 30 sec. Melting curve analysis was conducted following each real-time PCR and analyzed using the $2^{-\Delta\Delta Ct}$ method.[14] β-Actin was used as a reference gene because it is one of the most common housekeeping genes for normalizing gene expression levels, and its transcription level remains relatively constant in reaction to experimental

manipulation within the maximum tissues.[15] Changes in gene expression have been calculated from the acquired cycle threshold (Ct) values furnished through real-time PCR instrumentation using the comparative CT technique to a reference (housekeeping) gene (β-Actin).[16]

Ultrastructure of the cerebral cortex

Transmission electron microscopy (T.E.M) processing

Four blocks 1 x^2mm was taken from each sample immediately after animal dissecting and fixed in cold glutaraldehyde (5%) for 24–48 h. The specimens were then washed 3–4 times in cacodylate buffer (pH 7.2) for 20 min every time and post-fixed in osmium tetroxide (OSO_4) solution 1% for 2 h after that washed in the same buffer four times. Dehydration was done by ascending grades of alcohol (30 – 50 – 70 – 90 and 100%) for 2 h then embedded in epon–araldite mixture according to Winey et. al.[17] From the embedded blocks, semi-thin sections using LKB ultramicrotome in a thickness of 0.5–1μ were prepared for orientation of the tissue and photographed by SC30 Olympus Camera and then ultrathin section in a thickness of 500–700 A was made using Leica AG ultramicrotome and contrasted in uranyl acetate and lead citrate, as usual. The sections were examined using JEM-100 CXII transmission electron microscope at 80kv and photographed by CCD digital camera Model XR-41.

Statistical analysis

Data were expressed as mean± standard deviation (SD). Statistical analysis was performed between the control at 0-time and different time's postmortem groups using ANOVA followed by Duncan's multiple range test.[18] Differences were considered significant at P<0.05 level using SPSS for Windows (Version 20.0; SPSS Inc., Chicago, Ill).

Results

Changes in the brain oxidant/antioxidant parameters

In the brain tissue of the postmortem groups, the CAT and SOD activities and GSH level decreased significantly from the 2nd to 6th hpm (G3 to G6) when compared with the first group (at the time of death). Moreover, the MDA levels a marker of lipid peroxidation- were significantly increased at the 4th and 6th hpm (G4 and G5) when compared with 0, 1st and 2nd hpm (G1, G2, and G3) (Table 1).

RNA integrity in brain tissue

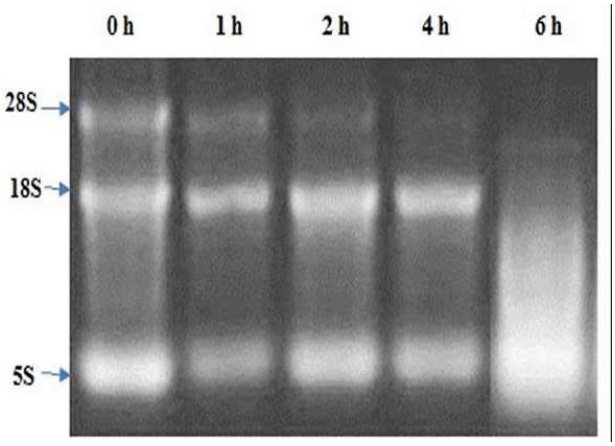

Fig. 1: Total brain RNA extracts during postmortem intervals. Total RNA extracts from dead rat brain electrophoresis in agarose gel (stained with ethidium bromide). The28S-rRNA bands lowered with the increase postmortem interval.

Total RNA became efficiently extracted from all rat samples. The mean RNA yield of brain tissue was 576 ng/mg (ranged 249–1187 ng/mg). The degradation profile of the total RNAs was evaluated during the postmortem interval and become assessed by electrophoresis in agarose gel. The amount of 28S-rRNA of rat brain at various postmortem durations declined gradually inside the PMI (Fig. 1). It was apparent that the control group (0 h) had three clear bands: 28S, 18S, and 5S,

Table 1: Oxidant/antioxidant markers in the rat's brain homogenates along the time of the experiment. (mean±SD, n=7).

Parameters	Time of death (hours)				
	0	1	2	4	6
Catalase (U/mg protein)	66.66±2.56[a]	25.55±2.58[b]	16.14±6.13[c]	8.62±0.80[d]	5.28±0.37[d]
SOD (U/mg protein)	1.28±0.12[a]	0.70±0.12[b]	0.36±0.03[c]	0.25±0.03[c]	0.03±0.01[d]
GSH (U/mg protein)	1.12±0.12[a]	0.95±0.07[b]	0.51±0.06[c]	0.28±0.04[d]	0.18±0.02[d]
MDA μmol/mg protein)	0.86±0.16[c]	1.16±0.08[c]	1.73±0.05[c]	3.41±0.52[b]	5.51±1.29[a]

Means with different superscripts in the same row are significantly different at P< 0.05.

SOD= Superoxide dismutase. GSH= Reduced glutathione. MDA= Malondialdehyde.

then the bands of 28S-rRNA reduced with growing postmortem interval time in G5 (6 hpm).

The control group (0 h) showed three clear bands, and the band depth of 5S changed into twice the other two bands. After 1st hpm, G2 showed that the three bands' intensities had been weaker than that of the control group, especially the 28S band. It changed into equal exchange from the 4th hpm until the 6th hpm in G4 and G5. The band intensity of 28S reduced to be nearly invisible, and the bands after 6th hpm (G5) degraded to be like a comet. The bands of 28S-rRNA reduced with the longer PMI.

RT-qPCR

The mean relative brain GAPDH-mRNA degrees after the different time intervals within the studied groups were proven in Fig. 2. The mean GAPDH-mRNA levels after the special studied postmortem interval time confirmed significantly reduced in G1 and G5, while the GAPDH ranges confirmed non-significant variations in the other three groups.

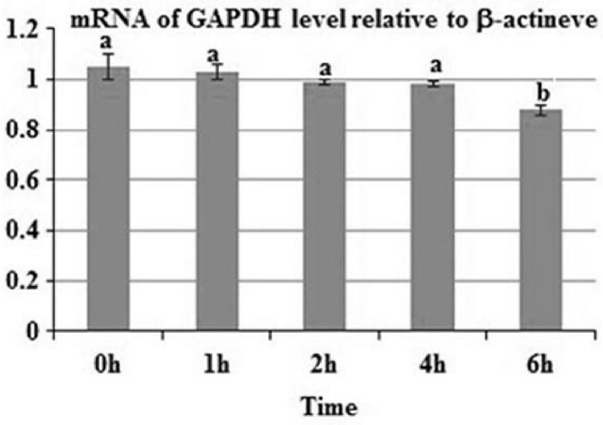

Fig. 2: Effect of postmortem interval on mRNA expression levels of the GAPDH gene in the brain tissue of rats.Mean values with different letters were significantly different at P≤0.05.

Transmission electron (T.E.) micrograph of the cerebral cortex

Postmortem Ultrastructure changes on nerve cells (Fig. 3).

At the time of death (0 h), (G1) showing the presence of large vesicular nucleus (N) containing prominent electron dens nucleolus (ne), nuclear sap informs of fine electron dense granules (X) and the nuclear chromatin small clumped attached to the nuclear membrane (arrow). The cytoplasm of the cell is rich with cell organelles such as free ribosomes (r), mitochondria (m), lysosomes (arrow), and rough endoplasmic reticulum (RER) (er). Also, surrounding the body of the nerve cell, processes of the glial cells and nerve axons containing cell organelles (XX) were noticed (Fig. 3a). On the 1st hpm (G2) showing evidence of lyses of the nuclear sap (x), shrinkage of the nucleolus (ne) and partial lyses of the nuclear membrane of the nerve cell (arrow). The cell cytoplasm contained contracted electron dens mitochondria (m), numerous electron dens lysosomes (arrow head) and numerous variable size vacuoles (v). The surrounding cell processes, as well as nerve axons containing electron dens mitochondria (m) with dispersion of the neurofilaments (x), were detected (Fig. 3b). On the 2nd hpm (G3), showing the nucleus (N) of the nerve cells having an irregular outline, shrinkage contained small electron dense granules. The cytoplasm contained numerous vacuoles (v), electron dense granules (arrow) and the mitochondria (m) became light electron dense. Also, the cell organelles of the cell processes appeared homogenous and electron dense (XX) were seen (Fig. 3c). At 4th hpm (G4), showing lyses of the nuclear chromatin (N), presence of homogenous electron dens nucleolus (ne) with partial loss of the nuclear membrane and the cytoplasm contained variable size and shape vacuoles (v) and electron-dense granules (arrow) (Fig. 3d). On the 6th hpm (G5), showing cytolyses of the nucleus and cytoplasm and appeared lost their detailed structures and became light electron dense with the presence of electron dense granules (arrow) and vacuoles (V). Also, lyses of the surrounding glial cell processes (X) and myelinated nerve axons and their myelin sheath (XX) were noticed (Fig. 3e).

Postmortem Ultrastructure changes on the nerve axon (Fig. 4).

At 0-hpm, (G1) showing the nerve axons of unmyelinated fiber (1) and myelinated nerve fiber with electron dens myelin sheath (2) contained neurofilament (x) and mitochondria (m). The cell process of the glial cells surrounding the nerve axons having normal cell organelles (XX) was observed (Fig. 4a). On the 1st hpm (G2), partial lyses of the myelin sheath of the myelinated nerve fiber (arrow) and the unmyelinated axons (x) were seen. Also, the mitochondria (m) of the axons and cell processes lost its membranous structure and became homogenous (Fig. 4b). The changes on 2nd hpm (G3), showing a variable degree of disorganization of the myelinated nerve fibers (X). Most of the cell organelles of the glial cell processes and nerve axons especially mitochondria (m) showing lyses, and light electron dense or

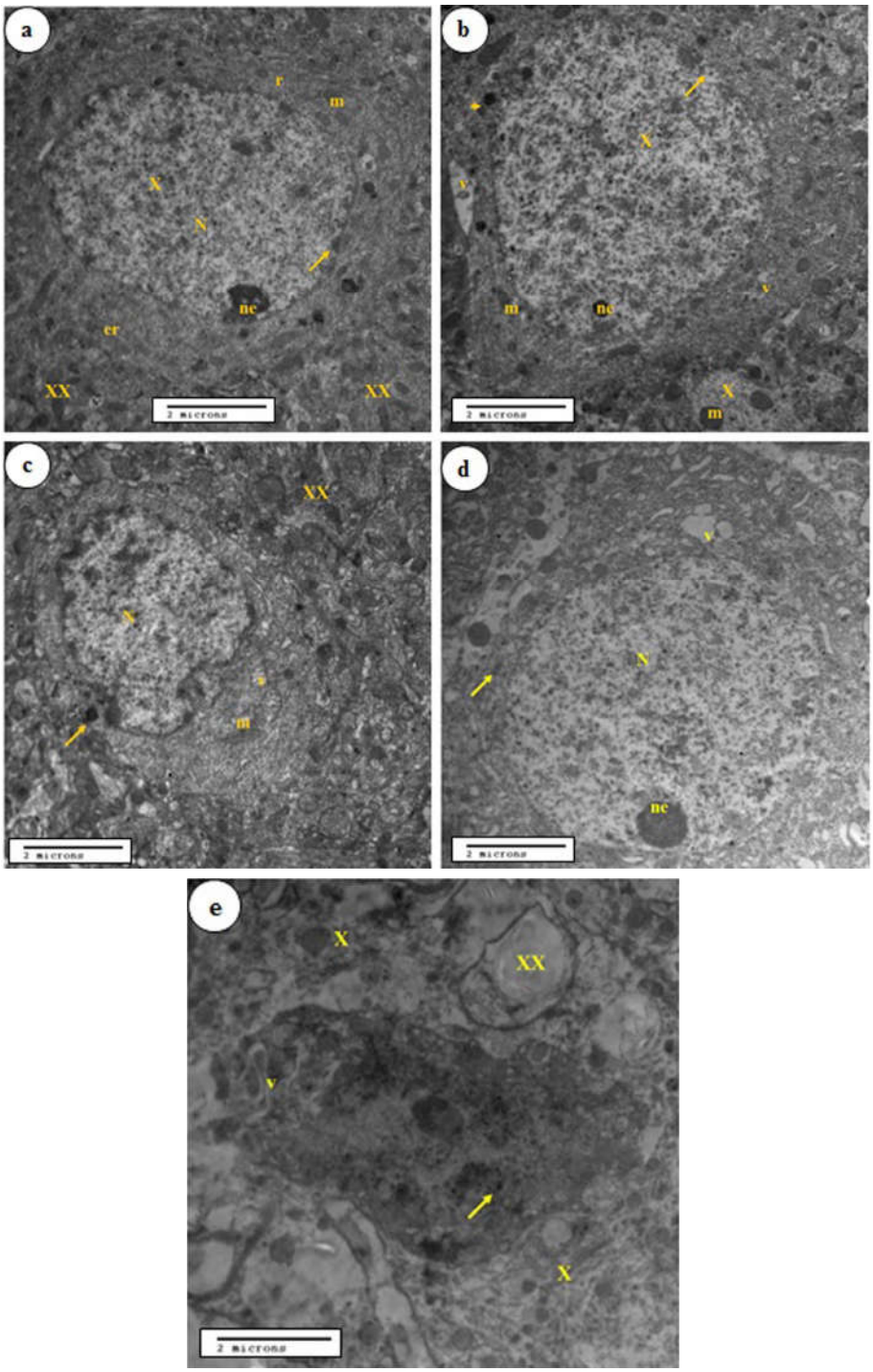

Fig. 3: Ultrastructure of early postmortem changes in nerve cells of rat's brain.

fragmented were detected (Fig. 4c). On the 4th hpm (G4), showing marked lyses of the myelin sheath (X) and vacuolation (V) of the myelinated nerve fiber. The unmyelinated nerve axons (XX) and glial cell processes showing lyses of the cell organelles with the presence of numerous electron dense lysosomes (arrow) (Fig. 4d). Finally, On the 6th hpm (G5), showing marked lyses of the umyelinated nerve axon (X) and marked disorganization and lyses of the glial cell processes (XX) with the presence of small electron dense granules (arrow) (Fig. 4e).

Postmortem Ultrastructure on the blood vessels (Fig. 5).

At 0-hpm (G1) showing the blood vessel lined with endothelial cells filled with blood plasma

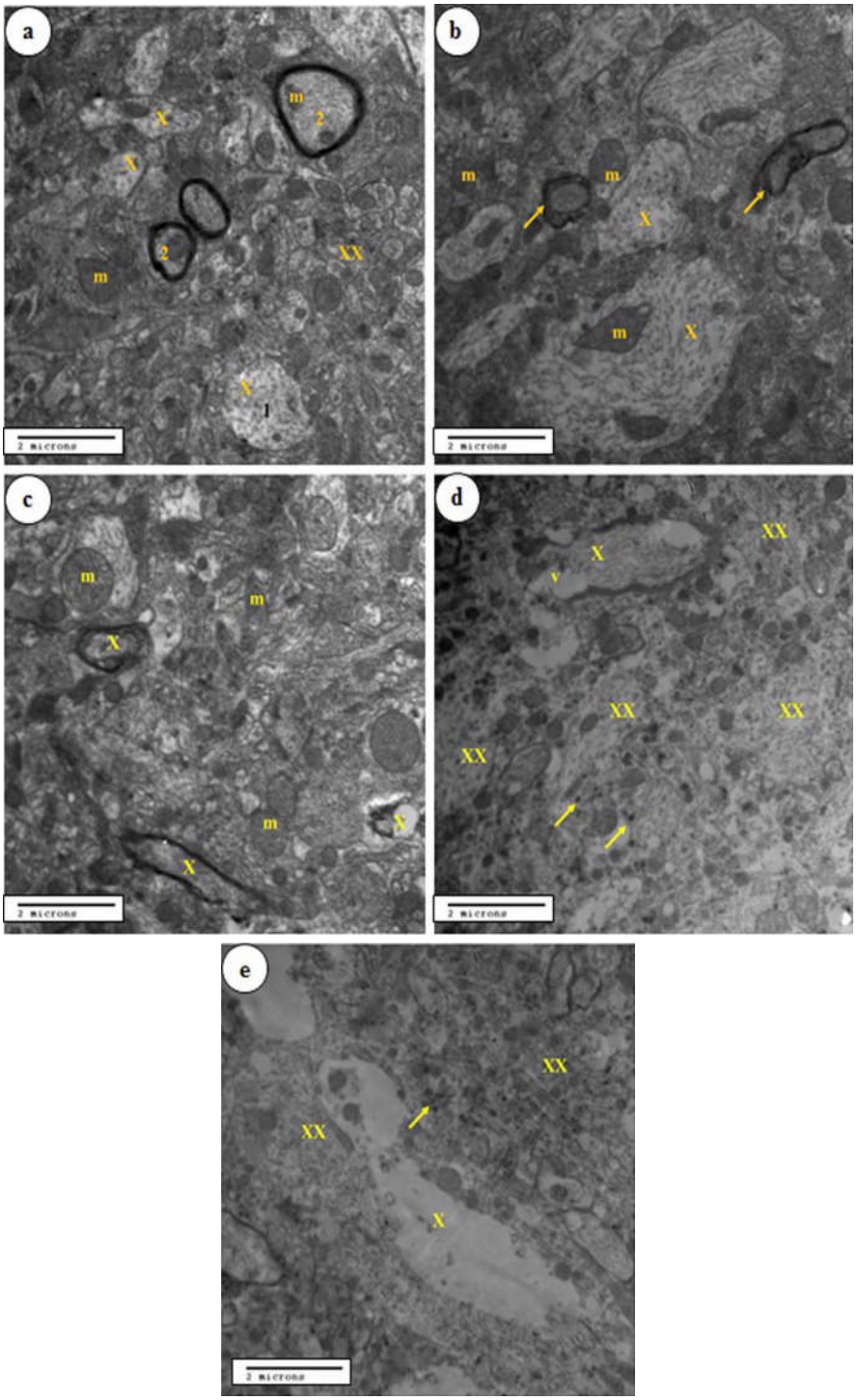

Fig. 4: Ultrastructure of early postmortem changes in nerve axon of rat's brain.

(x) and RBCs (rc). The nerve axons (1) and cell processes of glial cells (XX) were noticed closely attached to the blood vessel (Fig. 5a). While on the 1st hpm (G2), showing the wall of the blood vessel degenerated (X) and surrounded by empty spaces or vacuoles (v). Partial lyses of the nerve axon with the presence of small electron dense granules in the unmyelinated nerve fiber (arrow) were observed. The presence of numerous small electron dense bodies (arrow) and the mitochondria (m) of the cell processes lost its membranous structures with the presence of numerous vacuoles in the processes (XX) (Fig. 5b). The changes at the 2nd and 4th hpm (G3 and G4), showing degeneration of the blood vessel wall (X) and surrounded by empty spaces or large vacuoles (v). The organelles of the cell

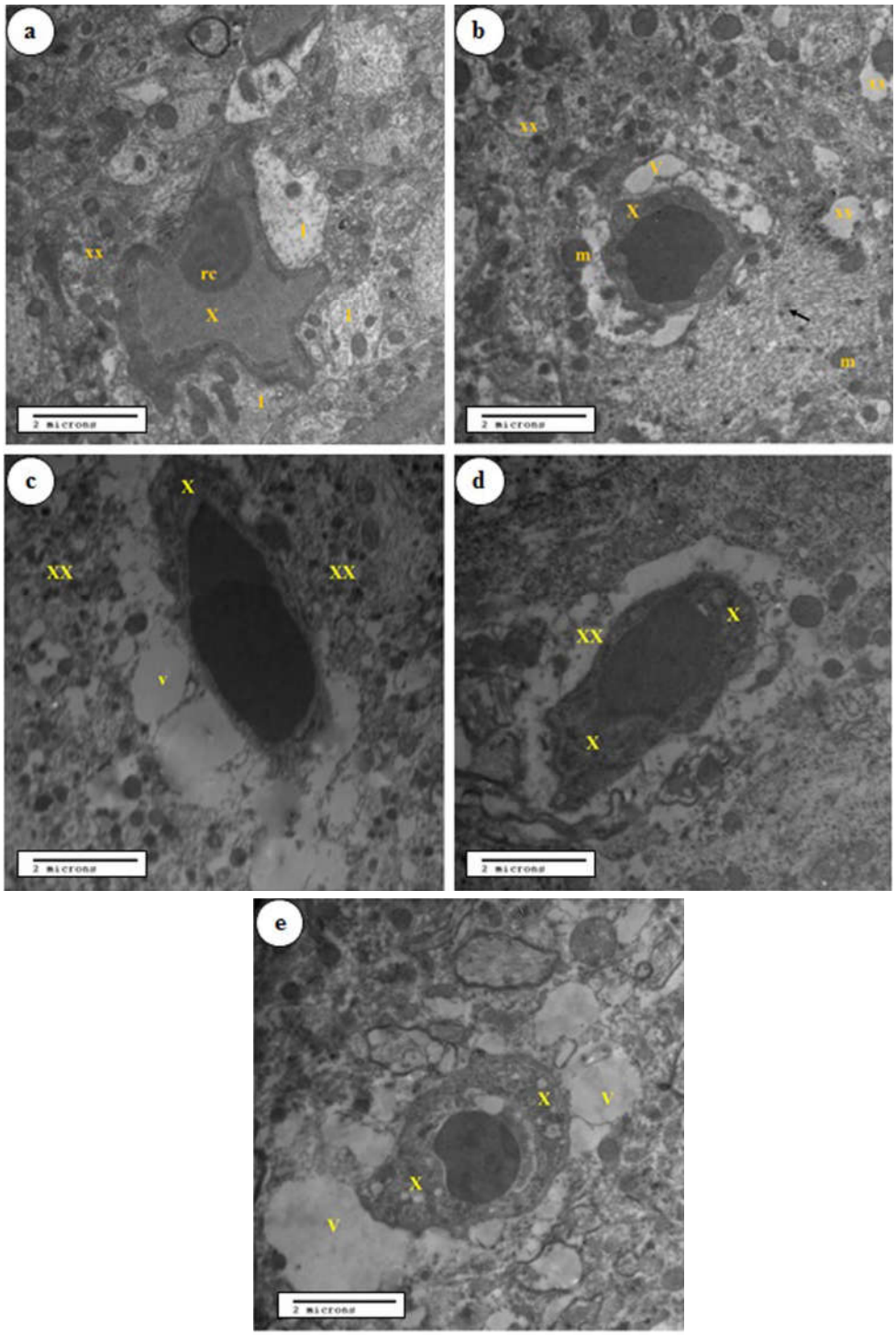

Fig. 5: Ultrastructure of early postmortem changes in blood vessels of rat's brain.

processes and nerve axons became disorganized and lyse with the presence of variable size electron dense granules or fragments (xx) (Fig. 5c and d). Finally, at the 6th hpm (G5), showing shrinkage and prominent degenerative changes of the wall of the blood vessel (X) and surrounded by empty space or vacuoles (V) (Fig. 5e).

Discussion

The present work was designated to record the biochemical, molecular and histopathological changes in rat's brain during the early 6 hours after death (at 0-h, 1st, 2nd, 4th, and the 6th hpm). The oxidant/antioxidant markers, RNA integrity, and

changes in the cell organelles using an electron microscope were assessed.

Thanatochemistry is the chemistry of death used for the description of the progressions that occur in the chemical composition of the human corpse immediately after death. The PMI is defined as the time passed since the death of an individual and refers to the stages of autolysis.[1] A precise estimation of the PMI requires the assessment of the parameters that change constantly with time after death. This definition fits well in postmortem changes of biochemical parameters since each change has its own time factor.[3]

After death, a drop in the concentration of oxygen (anoxia) is the most immediate biochemical change. It is due to the absence of circulation that resulting in a switch to anaerobic metabolism with the absence of the citric acid cycle. In the early postmortem period, there is a continuation of biochemical changes. In addition, the distribution of easily diffusible substances between erythrocytes and plasma as well as between interstitial fluid, tissue cells, and the blood were recorded.[19] The oxidant/antioxidant defense system in the human body is characterized by the formation of free radicals and their removal by means of the antioxidant systems. Increase the oxidant levels and decrease the antioxidant levels were observed in the damaged tissues.[20]

In the brain tissue, MDA started to increase significantly from the 4th till the 6th hpm. The increased MDA levels with increasing PMI are attributed to increased lipid peroxidation which in turn leads to increased binding and detoxification by GSH that is eventually reduced. These results were in accordance with Shaaban et. al.[20] These findings also agree with Ozturk et. al.[21] in a similar study on rat femoral muscle, who recorded that the MDA displayed a significant increase in contrast to antioxidants markers (CAT, SOD, and GSH), which showed a significant decrease during the 2nd to the 5th hpm. The amount of MDA is increased in parallel to the increase in the extent of damage in the experimental animal studies.[22] Moreover; the average increase of MDA in an experimentally damaged tissue has not been greatly different from that observed during further hours after death. Cell death increased the free radicals (oxidative stress) that could lead to the autolysis process.[5]

In the current study, the values of CAT were found to be significantly decreased at the 1st, 2nd and 4th hpm in the brain tissue. These results agree with those of Shaaban et. al.[20] who recorded that the CAT values be significantly decreased at the 3rd to 4th hpm in the brain tissue. Shaaban et. al.[20] found that the decrease in CAT level in rat liver became a significant decrease at the 1st to 2nd hpm. Catalase breaks hydrogen peroxide down into O and H2O using either an iron or manganese cofactor; in the brain, the CAT level is very low in comparison with other tissues.[23] It was hypothesized that the low activity of CAT in the brain is partially responsible for the high sensitivity of this organ to oxidative injury.[24] The results of the present study disagree with those of Harish et. al.[25] who stated that in human brain tissue there is no obvious alteration in the activity of CAT with increasing PMI.

In the present study, SOD and GSH values started to decrease significantly at the 1st and 2nd hpm in the brain. These findings agree with Shaaban et. al.[20] and disagree with those of Harish et. al.[25] who measured SOD activity in human brain tissue and showed no significant alteration with increasing PMI. In fact, the SOD is high at the time of death (0-hpm). It may be due to an aerobic medium in the brain is adequate for SOD to apply its antioxidant activity in this hour, later when enzymatic degradation by lytic enzymes starts in the brain, SOD starts to decrease. The GST catalyzed the reactions of toxic substances through conjugation with GSH protecting the cells from oxidative damage. Glutathione it is the crucial enzyme to maintain the cells from oxidative damage.[4] The difference in the enzyme responses may be in part due to the differences in the nature, amount, and activities of these enzymes in the tissues. The low activity of some antioxidant enzymes in the tissues was leading to tissue damage, damage of enzymatic structure, function, and gene expression.[26]

In this study, four different postmortem time intervals were examined (1, 2, 4. and 6 hpm) in addition to the fresh tissue at zero interval (0 h). In all studied groups, the brain GAPDH mRNA mean expression values decreased with growing PMI. These findings coincide with those of Inoue et. al.[27] who noticed that the Ct values for GAPDH mRNA in the rat brain increased linearly with PMI. Also, the adjustments of Ct values of brain β-actin mRNA of rats confirmed a good linear relationship with PMI at temperature 20°C.[28] In addition, the Ct values of GAPDH mRNA and β- actin mRNA of rat's brain measured by using real-time RT-PCR correlated well with the PMI recorded by way of Hunter et. al.[29] Elghamry et. al.[30] observed that the decrease of GAPDH mRNA levels with increasing PMI in the brain tissue of albino rats. Our results revealed significant negative correlations between GAPDH expression and postmortem time intervals, inside the G1, G2, G3, and G4. This may be due to

RNA from postmortem brain is more stable than RNA from postmortem of other tissues. A similar result was recorded some organs like pancreas and liver exhibit rapid RNA fragmentation due to the fact those organs contain considerable ribonuclease, the enzymatic activity activated at once after body death, and RNA degraded rapidly, whereas other tissues like brain and heart show much more balance up to ninety-six hpm.[31] Therefore, it's feasible that the stability of mRNA is adequate for postmortem evaluation, even if a dead body is left for numerous days at room temperature. Many mRNA markers had been studied for postmortem interval determination, including β-actin, and GAPDH.[32] These genes had been used as housekeeping genes in preferred molecular biology experiments and used as endogenous reference genes in qRT-PCR information evaluation but, they showed a close relationship with postmortem interval in PMI determination; it's unsuitable to be used as endogenous reference markers in our study. The decrease brain GAPDH mRNA mean expression values with increasing PMI may be attributed to the fact that RNA is degraded after death by means of ribonucleases already present inside the cells and/or originating from bacteria or other environmental contamination additionally, the consequences of the environmental elements including pH, UV light and humidity.[33] Hunter et. al.[29] reported significant loss of individual mRNA transcripts by increasing PMI.

In the present study, there were postmortem ultrastructure changes on nerve cells, nerve axons, and blood vessels. The changes on the nerve cells were involved in the nucleus, nucleolus, nuclear sap, and cytoplasm; there were cytolyses of the nucleus and cytoplasm with the presence of electron dense granules and vacuoles on the 6th hpm. The changes on nerve axons were involved in the myelin sheath of the myelinated and unmyelinated nerve fiber, and mitochondria of the axon; that appear normally at the time of death, but on the 6th hpm there were marked lyses of the unmyelinated nerve axon and the glial cell processes. The changes on the blood vessels have involved in the wall of the blood vessels and its surround tissues; there were shrinkage and prominent degenerative changes in the wall of the blood vessel that was surrounded by empty space or vacuoles at 6th hpm. These findings were agreed with Sheleg et. al.[34] who was studded the postmortem changes in rat's cortical neurons.

Ultrastructure changes in the present study were attributed to the anoxic post mortem effects, which occur after death and make changes in enzyme activity and cellular structure.[35] The process of autolysis (alterations in size, shape, electron density, and localization of cell structures) caused a gradual loss of highly arranged structural organization of cells.[36] The autolytic enzymes proved in lysosomes of living cells cause the destruction of their own cell components after death. Those enzymes disintegrate intracellular material, including cell organelles, so the cytoplasm became homogenous with a loss of cell details.[35]

In the present study, the brain tissues of rats (cerebrum) were examined to disclose whether or not a significant association was present among levels of oxidant/antioxidant parameters and PMI (0, 1st, 2nd, 4th, and 6th hpm). The current study revealed gradual deterioration in the ultrastructure of the cerebrum, which matched in time with the expansion in oxidant levels and reduction in antioxidant levels. These findings were in agreement with Ozturk et. al.[21] who reported that the histopathological changes in rat femoral muscle were matched with the oxidant/antioxidant postmortem changes.

Conclusions

In this work, we provide different methods for determining the early postmortem interval time in forensic cases using the brain tissues. Oxidative/antioxidative markers, GAPDH-mRNA gene expression, and ultrastructure postmortem changes in the brain tissues could be helpful in determining the changes in the first 6th hpm at room temperature (25^{0}C) before the autolysis occur. Future investigations will be studies the factors affected in postmortem autolytic processes such as the cause and manner of death, temperature, air humidity, environmental conditions, more durationof up to 24 hours.

Recommendations

We recommended that the oxidative markers and the ultrastructure changes in brain tissues more realistic in determining the early postmortem interval time than RNA integrity and GAPDH m-RNA gene expression.

Acknowledgments

The authors are grateful to Professor Dr. Allam Nafady, Professor of Pathology, Faculty of Veterinary Medicine, Assiut University, Egypt, for his valuable support, and also thank the staff of the

Department of Forensic Medicine and Toxicology, Faculty of Veterinary Medicine, Benha University, Egypt, for their help. The authors did not receive any funding for this study.

Funding information: None.

Compliance with ethical standards

Conflict of interest: The authors declare that they have no conflict of interest.

Ethical approval: This experiment was carried out according to the guidelines of the Institutional Review Board for Animal Experiments at Benha University, Egypt, the Approval Protocol No.: (284/2019).

References

1. Peng D, Lv M, Li Z, et. al. Postmortem interval determination using mRNA markers and DNA normalization. Int J Legal Med. 2020;134(1): 149–157.
2. Elalfy MM, Ragheb HH, Hamed MF, et. al. Biochemical markers and pathological features of postmortem time interval distinguishing freshwater and saltwater drowning induced death in Albino rats. Biomed J Sci & Tech Res. 2019;20(1):14713–14720.
3. Li C, Wang Q, Zhang Y, et. al. Research progress in the estimation of the postmortem interval by Chinese forensic scholars. Forensic Sci Res. 2016;1(1):3–13.
4. da Fonseca CAR, Paltian J, Dos Reis AS, et. al. Na+/K+-ATPase, acetylcholinesterase and glutathione S-transferase activities as new markers of postmortem interval in Swiss mice. Leg Med (Tokyo). 2019;36:67–72.
5. Zaki AR, Tohamy AF, Yaseen NE. Estimation of postmortem intervals by some biochemical changes and DNA degradation in rat brain and skeletal muscle tissues. Mansoura Journal of Forensic Medicine and Clinical Toxicology. 2017;25(1):59–78.
6. Tu C, Du T, Shao C, et. al. Evaluating the potential of housekeeping genes, rRNAs, snRNAs, microRNAs and circRNAs as reference genes for the estimation of PMI. Forensic Sci Med Pathol. 2018;14(2):194–201.
7. Kim JY, Kim Y, Cha HK, et. al. Cell death-associated ribosomal RNA cleavage in postmortem tissues and its forensic applications. Mol cells. 2017;40(6):410–417.
8. Hegazy AM, Farid AS, Hafez AS, et. al. Hepatoprotective and immunomodulatory effects of copper-nicotinate complex against fatty liver in rat model, Vet World. 2019;12 (12):1903–1190.
9. Luck, H. A spectrophotometric method for the estimation of catalase. In: H.U. Bergmeyer (Editor). Methods of Enzymatic Analysis. New York: Academic Press;1963:886–887.
10. Misra HP, Fridovich I. The role of superoxide anion in the autoxidation of epinephrine and a simple assay for superoxide dismutase. J Biol Chem. 1972;247(10):3170–3175.
11. Ellman GL. Tissue sulfhydryl groups. Arch Biochem Biophys. 1959;82(1):70–77.
12. Ohkawa H, Ohishi N, Yagi K. Assay for lipid peroxides in animal tissues by thiobarbituric acid reaction. Anal Biochem. 1979;95(2):351–358.
13. Lowry OH, Rosebrough NJ, Farr AL, et. al. Protein measurement with the Folin phenol reagent. J Biol Chem. 1951;193(1):265–275.
14. Abdel-Aziem SH, Hassan AM, El-Denshary ES, et. al. Ameliorative effects of thyme and calendula extracts alone or in combination against aflatoxins-induced oxidative stress and genotoxicity in rat liver. Cytotechnology. 2014;66(3):457–470.
15. Paria A, Dong J, Babu PPS, et. al. Evaluation of candidate reference genes for quantitative expression studies in Asian seabass (Lates calcarifer) during ontogenesis and in tissues of healthy and infected fishes. Indian J Exp Biol. 2016;54(9):597–605.
16. Chapman JR, Helin AS, Wille M, et. al. A panel of stably expressed reference genes for real-time qPCR gene expression studies of mallards (Anas platyrhynchos). PLoS One. 2016;11(2):e0149454.https://doi.org/10.1371/journal.pone.0149454.
17. Winey M, Meehl JB, O'Toole ET, et. al. Conventional transmission electron microscopy. Mol Biol Cell. 2014;25(3):319–323.
18. Snedecor, G., Cochran, W. Statistical Methods. 8th ed., Ames, IA: Iowa State University Press; 1989:237–252.
19. Lv YH, Ma JL, Pan H, et. al. RNA degradation as described by a mathematical model for postmortem interval determination. J Forensic Leg Med. 2016;44:43–52.
20. Shaaban AAE, Farrag IM, Mostafa I, et. al. Estimation of early postmortem interval by biochemical changes in brain and liver of rats using some oxidant and antioxidant parameters. The Egyptian Journal of Forensic Sciences and Applied Toxicology. 2017;17(1):147–162.
21. Ozturk C, Sener MT, Sener E, et. al. The investigation of damage in the muscle tissue with the oxidant/antioxidant balance and the

extent of postmortem DNA damage in rats. Life Sci J. 2013;10(3):1631–1637.

22. Atasever M, Bakacak Z. Nigella Sativa oil protects the rat ovary from oxidative injury due to ischemia-reperfusion. Med Sci Monit. 2017;23:5027. https://doi.org/10.12659/MSM.905356.
23. Chelikani P, Fita I, Loewen PC. Diversity of structures and properties among catalases. Cell Mol Life Sci. 2004;61(2):192–208.
24. Abo El-Noor MM, Elhosary NM, Khedr NF, et. al. Estimation of early postmortem interval through biochemical and pathological changes in rat heart and kidney. Am JForensic Med Pathol. 2016;37(1):40–46.
25. Harish G, Venkateshappa C, Mahadevan A, et. al. Glutathione metabolism is modulated by postmortem interval, gender difference and agonal state in postmortem human brains. Neurochem Inter. 2011;59(7):1029–1042.
26. Ighodaro OM, Akinloye OA. First line defence antioxidants-superoxide dismutase (SOD), catalase (CAT) and glutathione peroxidase (GPX): Their fundamental role in the entire antioxidant defence grid. Alexandria J Med. 2018;54(4):287–293.
27. Inoue H, Kimura A, Tuji T. Degradation profile of mRNA in a dead rat body: basic semi-quantification study. Forensic Sci Int. 2002;130(2–3):127–32.
28. Elghamry HA, Mohamed MI, Hassan FM, et. al. Potential use of GAPDH m-RNA in estimating PMI in brain tissue of albino rats at different environmental conditions. EgyptJ Forensic Sci. 2017;7:24.https://doi.org/10.1186/s41935–017–0024–8.
29. Hunter MC, Pozhitkov AE, Noble PA. Accurate predictions of postmortem interval using linear regression analyses of gene meter expression data. Forensic Sci Int. 2017;275:90–101.
30. Elghamry HA, Hassan FM, Mohamed MI, et. al. Estimation of the postmortem interval using GAPDH mRNA in skin and heart tissues of albino rats at different environmental conditions. EgyptJ Forensic Sci. 2018;8:69. https://doi.org/10.1186/s41935–018–0102–6.
31. El-Harouny MA, El-Dakroory SA, Attalla SM, et. al. The relationship between postmortem interval and DNA degradation in different tissues of drowned rats. Mansoura J Forensic Med Clin Toxicol. 2008;16(2):45–61.
32. Lv YH, Ma JL, Pan H, et. al. Estimation of the human postmortem interval using an established rat mathematical model and multi-RNA markers. Forensic Sci Med Pathol. 2017;13(1):20–27.
33. Scrivano S, Sanavio M, Tozzo P, et. al. Analysis of RNA in the estimation of post-mortem interval: a review of current evidence. Int J Legal Med. 2019;133(6):1629–1640.
34. Sheleg SV, LoBello JR, Hixon H, et. al. Stability and autolysis of cortical neurons in post-mortem adult rat brains. Int JClin Exp Pathol. 2008;1(3):291–299.
35. Hostiuc S, Rusu MC, Manoiu VS, et. al. Usefulness of ultrastructure studies for the estimation of the postmortem interval. A systematic review. Rom J Morphol Embryol. 2017;58(2):377–384.
36. De-Giorgio F, Nardini M, Foti F, et. al. A novel method for post-mortem interval estimation based on tissue nano-mechanics. Int JLegal Med. 2019;133(4):1133–1139.